# New Methods for NMR of Cuprate Superconductors

J. Haase, N. J. Curro, R. Stern, and C. P. Slichter

*Department of Physics and Materials Research Laboratory, University of Illinois at Urbana-Champaign, 1110 West Green Street, Urbana, Illinois 61801-3080*

(Received 13 March 1998)

New nuclear magnetic resonance (NMR) methods for the investigation of high temperature superconductors are reported which alleviate many of the problems NMR faces in such materials. The methods rely on combining population transfers between quadrupolar split Zeeman levels with ordinary NMR experiments. Spins labeled in this manner can be investigated selectively, e.g., allowing the differentiation between isotopes, crystallographic sites, and misaligned grains. Examples for Cu NMR on $YBa_2Cu_4O_8$ and $La_{1.85}Sr_{0.15}CuO_4$ are reported. The methods will also be applicable to other areas of solid state NMR. [S0031-9007(98)06910-5]

PACS numbers: 74.25.Ha, 74.72.Bk, 76.60.Es, 76.60.Gv

Nuclear magnetic resonance (NMR) has contributed unique pieces of information about the physical properties and structure of superconductors [1–3]. The magnetic shift ($K_s$), the spin-lattice relaxation rate ($W_1$), and the Gaussian component of the spin-spin relaxation rate [4] ($1/T_{2G}$) are the most interesting parameters since they probe locally the electron spin susceptibility and the hyperfine interactions which allow important conclusions about theories of these materials [5,6]. However, we are still far from a complete understanding of the NMR results in a variety of materials. This is related to the fact that NMR experiments in these materials suffer frequently from overlapping resonance lines from (a) various isotopes, (b) different chemical sites, (c) different transitions of the same site, or (d) intrinsic line broadening. We report new NMR methods which alleviate these problems and illustrate with several examples.

The basic principle behind these new methods is simple. Many of the nuclei in high temperature superconductors are nuclei with a quadrupole moment such as $^{63,65}$Cu ($I = \frac{3}{2}$), $^{17}$O ($I = \frac{5}{2}$), $^{139}$La ($I = \frac{7}{2}$), $^{135,137}$Ba ($I = \frac{3}{2}$). For these nuclei the quadrupole interaction typically dominates all other interactions, except for the Zeeman term (in magnetic fields of several tesla). As a consequence, the $2I + 1$ Zeeman levels are considerably shifted by the quadrupole interaction [7] so that the resonances of the nuclei occur over a large frequency range. On the other hand, any radio frequency (rf) pulse which we use for signal detection has a much smaller bandwidth. Therefore, such pulses will change populations or create coherences in a relatively narrow frequency range. However, since neighboring transitions share one energy level, any pulse on a given transition will also affect the population difference of the neighboring transition regardless of the frequency difference between the two transitions. In fact, for a system initially at thermal equilibrium an arbitrary pulse at one transition will increase the population difference of the neighboring transition. A selective $\pi$ pulse will indeed double the population differences in the neighboring transition [8].

In short, we use double resonance methods to induce changes in the thermal equilibrium populations of the spin system at the resonance frequency of one transition and observe the changes in a neighboring transition at a second frequency. By subtracting the signal without such a transfer from the signal with a preceding transfer we obtain just the signal from the transferred spins (signal accumulation in add/or subtract mode). The time between the transfer pulse and the pulses for detection must be comparable to or shorter than the spin-lattice relaxation time so that the effect of the transfer pulse still persists when the signal is observed. We then use these transferred (labeled) spins to perform further experiments.

All examples shown concern the central $(\frac{1}{2}, -\frac{1}{2})$ and high frequency satellite transition $(\frac{3}{2}, \frac{1}{2}$ or $-\frac{3}{2}, -\frac{1}{2})$ of $^{63,65}$Cu isotopes at room temperature in the magnetic field of 8.3 T using a homebuilt NMR spectrometer. The crystal $c$ axis for the oriented powders of $YBa_2Cu_4O_8$ (YBCO, 1248) and $La_{1.85}Sr_{0.15}CuO_4$ (LSCO) was parallel to the applied field.

Let us address the YBCO family of materials first. Since large single crystals of YBCO are hard to obtain, most NMR measurements are done on oriented powder samples. Typically, the grain alignment is no better than within a few degrees, resulting in an asymmetric NMR line with a low frequency tail. Moreover, YBCO contains two chemically inequivalent coppers (chains and planes) and the NMR lines from these sites overlap for most of the accessible field strengths. This situation is depicted in the inset of Fig. 1 for a 1248 sample, where we show schematically the $^{63}$Cu resonances in two frequency ranges: (a) 92–97 MHz and (b) 123–126 MHz. Range (a) is most important since the $^{63}$Cu(2) central transition of the copper from the conducting planes falls in this range. However, as the inset shows, the $^{63}$Cu(1) signals from the chains, central and both satellite transitions, fall also in this frequency range and mask the $^{63}$Cu(2) signal. This complicates essentially the accurate estimation of $K_s$ [9] and the measurements of both $W_1$ [10] and $T_{2G}$. We now use the

  

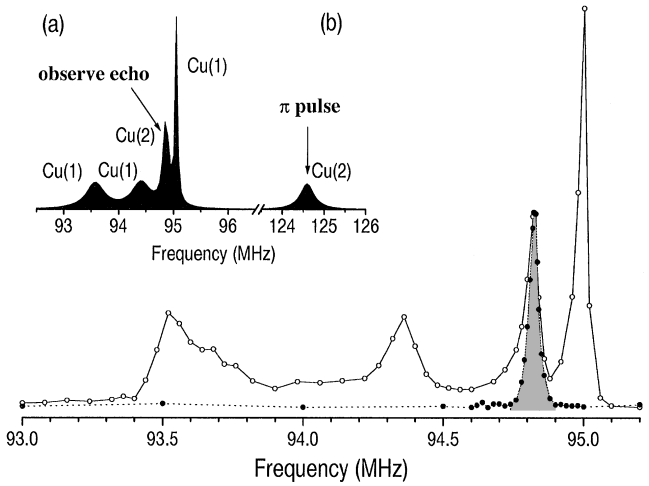


FIG. 1. $^{63}$Cu NMR spectra of $YBa_2Cu_4O_8$. Inset: schematic ordinary NMR spectrum of $^{63}$Cu in two frequency ranges (a) 92 to 97 MHz and (b) 123 to 126 MHz showing the overlap of the Cu(2) central transition with three Cu(1) lines in region (a). The region (b) shows the Cu(2) satellite transition. Main figure: ○, the $^{63}$Cu spectrum for a conventional spin echo; ●, the Cu(2) spectrum produced by the new method using $\pi$ pulses at the Cu(2) satellite line. Note both the elimination of overlapping Cu(1) lines and the narrowing of the Cu(2) line.

well-separated $^{63}$Cu(2) satellite transition signal in the frequency range (b) to increase the resolution for the $^{63}$Cu(2) central transition. As indicated in the inset, we apply a $\pi$ pulse to the planar $^{63}$Cu satellite at 124.6 MHz, then excite a spin echo in range (a). A second spin echo without the 124.6 MHz transfer pulse is then subtracted from the first spin echo. The resulting intensity versus frequency is plotted in the main part of Fig. 1. The resolution enhancement is striking; we can clearly differentiate between plane and chain copper (similar results can be obtained with the less abundant $^{65}$Cu isotope). The observed linewidth for the $^{63}$Cu(2) central transition of 33 kHz can compare with that of one of our single crystal of $YBa_2Cu_3O_7$ which has a linewidth of 42 kHz (large enough single crystals for $YBa_2Cu_4O_8$ are hardly available).

The same technique was applied for recording the line shape of the $^{63}$Cu(2) satellite transition: The transfer pulse was applied at the central transition frequency of the planar $^{63}$Cu at 94.825 MHz and the satellite transition was observed in the add/subtract mode. The resulting line shape (not shown) was much narrower compared with that obtained with a simple spin echo technique which is due to the fact that we eliminated much of the spectrum from misaligned crystals. This narrower satellite line shape now agrees quite well with that of nuclear quadrupolar resonance (NQR), where there is no alignment problem since the static field is zero.

In our second example, we address the LSCO family of cuprates, which are relatively simple single layer compounds, yet their normal state properties are not well understood. One peculiarity with the system is the occurrence of two different crystallographic Cu sites ($A$ and $B$) which have been found by NQR [11,12]. Site $A$ already occurs in the pure ($x = 0$) material, site $B$ arises when $x \neq 0$. In fact, more evidence accumulates showing that stripes might occur in these materials [13–15]. A complete understanding of the NMR in $La_{2-x}Sr_xCuO_4$ compounds has not been reached mainly due to resolution problems, e.g., due to the misalignment of grains and the great similarity of the two sites $A$ and $B$ [16–20]. A similar situation is met with the oxygen doped $La_2CuO_{4+\delta}$ materials [21,22].

We demonstrate in Fig. 2 how our new methods help us differentiate between the two Cu sites $A$ and $B$, the two $^{63,65}$Cu isotopes, as well as misaligned grains for $La_{1.85}Sr_{0.15}CuO_4$.

The central transitions of both Cu isotopes (not shown) are well separated due to the difference in their gyromagnetic ratios (94.7 MHz and 101.5 MHz at 8.3 T); however,

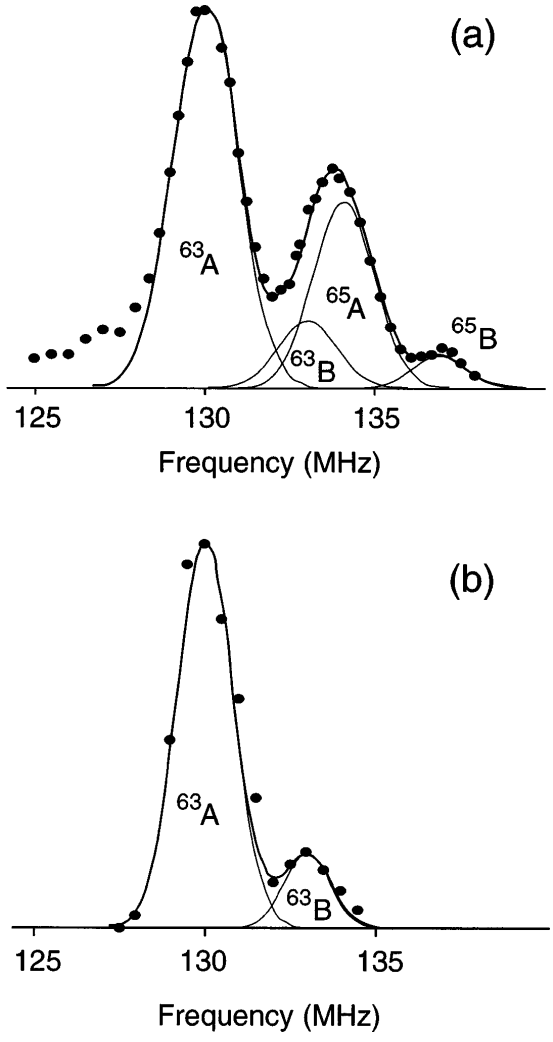


FIG. 2. Satellite resonances of $La_{1.85}Sr_{0.15}CuO_4$. (a) Obtained by an ordinary spin echo technique and fitted by four Gaussians (two isotopes and two crystallographic sites $A$ and $B$). (b) With population transfer from the $^{63}$Cu central transition at 94.7 MHz, fitted by two Gaussians.

the signals from the Cu $A$ and $B$ sites cannot be resolved in the central transition of either isotope. On the other hand, the satellite transitions are a superposition of all isotopes and sites [Fig. 2(a)]. We see a spectrum which we attempt to fit with four Gaussians for the two sites ($A$ and $B$) and two isotopes. To obtain Fig. 2(b), we observe spin echoes (in add/subtract mode) in the satellite frequency range, alternately applying a transfer pulse at the $^{63}$Cu central transition. It is seen that the ordinary satellite spectrum collapsed to a single isotope spectrum similar to those which can be achieved by an expensive isotope enrichment [23]. In addition, we can differentiate between signals from less well aligned parts of the sample [note the absence, in Fig. 2(b), of the long low frequency tail of Fig. 2(a)].

To separate the $A$ and $B$ spectra of the central transition of either isotope, we use the resolved spectra of the satellite [see Fig. 2(b)] to choose a frequency for population transfer and observe spin echoes near the $^{63}$Cu central transition in the add/subtract mode. The results are shown in Fig. 3. Note that, although the $A$ and $B$ spectra lay on top of each other, we can still plot out each one separately.

In a third example, we address $W_1$ and $T_{2G}$ measurements in the $La_{2-x}Sr_xCuO_4$ cuprates to explain how our methods, for the first time, enable us to measure these quantities for both isotopes and both sites $A$ and $B$. As already mentioned, the two Cu sites $A$ and $B$, misaligned grains, and overlapping isotopes introduce many uncertainties for data analysis [18–20]. This is part of the reason why, e.g., the understanding of $T_{2G}$ in these materials could not be fully achieved. However, using our population transfers, we can now measure these parameters for the $A$ and $B$ sites separately. In order to obtain $W_1$ we again observe the central transition, subtracting signals without population transfer from those with population transfer at the satellite frequency, but as a function of the delay between the transfer pulse and the spin echo for observation. In this way we can observe the decay of the polarization of the labeled spins (see Fig. 4) (note that the decay of the polarization follows the usual $W_1$ normal modes [24] with the initial condition that the thermal equilibrium populations of the $m = \frac{1}{2}$ and $\frac{3}{2}$ states are interchanged). We find that the relaxation rates for both sites are different, which is in agreement with NQR data [23] obtained with an isotope enriched sample.

Another piece of important information obtainable by our selective $W_1$ measurements is the existence or absence of spin diffusion or mutual spin flips. By using frequency selective transfer pulses, especially on the wider satellites, we can probe the behavior of a subset of spins. In case of spin diffusion their polarization decay would be much faster than that given by $W_1$. From our experiments we found no evidence of fast mutual spin flip processes [20,25].

Similar to the $W_1$ measurements, we can measure the spin echo decay of a selected part of the spin system by varying the delay between the $\frac{\pi}{2}$ and $\pi$ pulse. We show in Fig. 5 the spin echo decays of the total central transition (at the line maximum) and the corresponding $A$ and $B$ sites, which previously could not be measured.

We infer from Fig. 5 that the decay curves for the two sites are quite different. However, due to the rather short

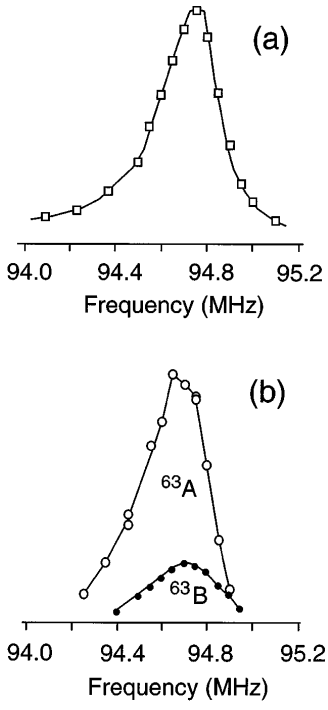


FIG. 3. $^{63}$Cu central transition of $La_{1.85}Sr_{0.15}CuO_4$. (a) Recorded with an ordinary spin echo technique. (b) Signals with population transfer at 130.0 MHz (○) for the $^{63}$Cu $A$ site and 133.1 MHz (●) for the $^{63}$Cu $B$ site.

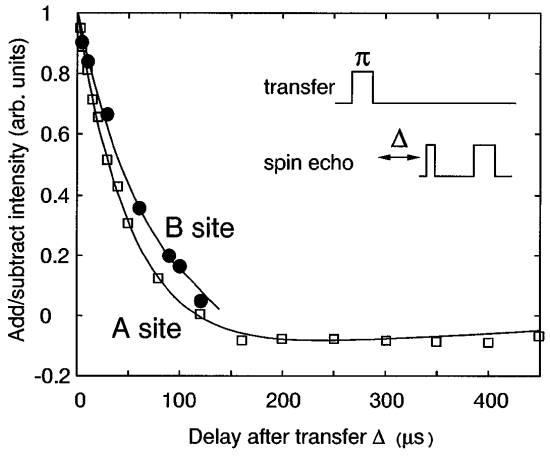


FIG. 4. NMR spin-lattice relaxation of the $A$ and $B$ site $^{63}$Cu in add/subtract mode with transfer at 130.0 MHz and 133.1 MHz, respectively. Fits to the decay according to $I(\Delta) = -\frac{1}{5}\exp(-\frac{2}{3}W_1\Delta) + \frac{6}{5}\exp(-4W_1\Delta)$ with $W_{1A}^{-1} = 220\ \mu$s and $W_{1B}^{-1} = 300\ \mu$s.

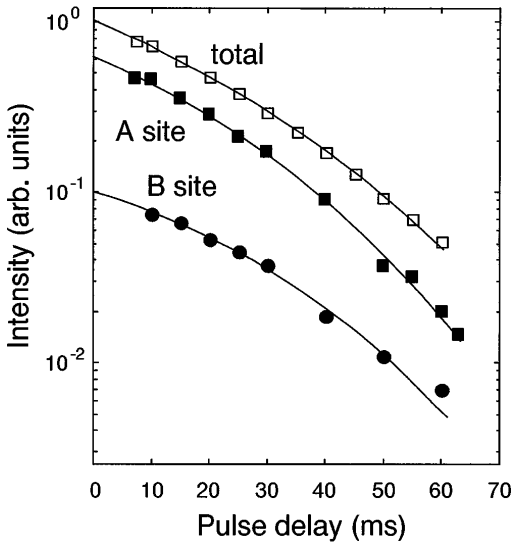


FIG. 5. $^{63}$Cu spin echo decays for the total central transition, the Cu *A* site, and the Cu *B* site. The solid lines represent $T_{2G}$ fits with $W_1$ corrections (see text). All data are measured at 94.7 MHz (maximum of the $^{63}$Cu resonance). For the *A* and *B* site data, population transfers were performed at 130.0 MHz and 133.1 MHz, respectively.

relaxation rates, we have to include $W_1$ corrections for the analysis of the spin echo decay [25]. Now, since we have already measured the relaxation rates separately (Fig. 4), the $T_{2G}$ analysis can be accomplished. Surprisingly, the *A* and *B* sites have the same $^{63}T_{2G}$ of 95 $\pm$ 4 $\mu$s. With analogous experiments for the $^{65}$Cu isotope we obtain a similar result, in that the $^{65}T_{2G}$ of both sites is the same, namely, 125 $\pm$ 5 $\mu$s. These results are the first site selective $T_{2G}$ measurements. The ratio for the two isotopes, $^{65}T_{2G}/^{63}T_{2G} = 125/95 = 1.32$, agrees well with the theoretically expected value [25] of 1.30.

In conclusion, we have demonstrated the utility of our new methods for NMR investigations of superconductors. For quadrupolar nuclei they can enhance the resolution by differentiating between different isotopes, different crystallographic sites, and misaligned sample material. In addition, there are many more applications in solid state NMR where our methods would help clarify structural aspects.

This work has been supported by The Science and Technology Center for Superconductivity under NSF Grant No. DMR91-20000 and the U.S. DOE Division of Materials Research under Grant No. DEFG02-91ER45439. J. H. acknowledges support from the Deutsche Forschungsgemeinschaft.

[1] L. C. Hebel and C. P. Slichter, Phys. Rev. **107**, 901 (1957); *ibid.* **113**, 1504 (1959).
[2] A. G. Redfield and A. G. Anderson, Phys. Rev. **116**, 583 (1959).
[3] D. E. MacLaughlin *Solid State Physics* (Academic Press, New York, 1976), Vol. 31.
[4] C. H. Pennington and C. P. Slichter, Phys. Rev. Lett. **66**, 381 (1991).
[5] C. P. Slichter, in *Strongly Correlated Electronic Materials*, edited by K. S. Bedell, Z. Whang, D. E. Meltzer, A. V. Balatsky, and E. Abrahams (Addison-Wesley, Reading, MA, 1993), p. 427.
[6] Special issue on containing contributions of NMR/NQR work in cuprate superconductors, edited by M. Mehring [Appl. Magn. Reson. **3**, 383 (1992)].
[7] C. P. Slichter, *Principles of Magnetic Resonance* (Springer Verlag, New York, 1990), 3rd ed.
[8] J. Haase, M. S. Conradi, C. P. Grey, and A. J. Vega, J. Magn. Reson. A **109**, 90 (1994).
[9] R. E. Walstedt, R. F. Bell, L. F. Schneemeyer, J. V. Waszczak, and G. P. Espinosa, Phys. Rev. B **45**, 8074 (1992).
[10] J. A. Martindale, S. E. Barrett, D. J. Durand, K. E. O'Hara, C. P. Slichter, W. C. Lee, and D. M. Ginsberg, Phys. Rev. B **50**, 13 645 (1994).
[11] K. Yoshimura, T. Imai, T. Shimizu, Y. Ueda, K. Kosuge, and H. Yasuoka, J. Phys. Soc. Jpn. **58**, 3057 (1989).
[12] K. Kumagai and Y. Nakamura, Physica (Amsterdam) **157C**, 307 (1989).
[13] D. Haskel, E. A. Stern, D. G. Hinks, A. W. Mitchell, and J. D. Jorgensen, Phys. Rev. B **56**, R521 (1997).
[14] J. M. Tranquada, J. D. Axe, N. Ichikawa, A. R. Moodenbaugh, Y. Nakamura, and S. Uchida, Phys. Rev. Lett. **78**, 338 (1997).
[15] A. Bianconi, N. L. Saini, A. Lanzara, M. Missori, T. Rossetti, H. Oyanagi, H. Yamaguchi, K. Oka, and T. Ito, Phys. Rev. Lett. **76**, 3412 (1996).
[16] Y. Q. Song, M. A. Kennard, M. Lee, K. R. Poeppelmeier, and W. P. Halperin, Phys. Rev. B **44**, 7159 (1991).
[17] Y. Q. Song, M. A. Kennard, K. R. Poeppelmeier, and W. P. Halperin, Phys. Rev. Lett. **70**, 3131 (1993).
[18] R. E. Walstedt, B. S. Shastry, and S. W. Cheong, Phys. Rev. Lett. **72**, 3610 (1994).
[19] R. E. Walstedt and S. W. Cheong, Phys. Rev. B **51**, 3163 (1995).
[20] R. E. Walstedt and S. W. Cheong, Phys. Rev. B **53**, R6030 (1996).
[21] P. C. Hammel, A. P. Reyes, E. T. Ahrens, D. E. MacLaughlin, J. D. Thompson, Z. Fisk, P. C. Canfield, S. W. Cheong, and J. E. Schirber, Physica (Amsterdam) **199B-200B**, 235 (1994).
[22] P. C. Hammel, Phys. Rev. B **57**, R712 (1998).
[23] Y. Itoh, M. Matsumura, and H. Yamagata, J. Phys. Soc. Jpn. **65**, 3747 (1996).
[24] E. R. Andrew and D. P. Tunstall, Proc. Phys. Soc. **78**, 1 (1961).
[25] N. J. Curro, T. Imai, C. P. Slichter, and B. Dabrowski, Phys. Rev. B **56**, 877 (1997).